ENVIRONMENTAL RESEARCH
LETTERS

LETTER • OPEN ACCESS

The effectiveness of net negative carbon dioxide emissions in reversing anthropogenic climate change

Environmental Research Letters

CrossMark

OPEN ACCESS

RECEIVED
9 July 2015

REVISED
23 August 2015

ACCEPTED FOR PUBLICATION
26 August 2015

PUBLISHED
10 September 2015

LETTER

The effectiveness of net negative carbon dioxide emissions in reversing anthropogenic climate change

Katarzyna B Tokarska and Kirsten Zickfeld

Department of Geography, Simon Fraser University, Burnaby, B.C., Canada

E-mail: tokarska@uvic.ca

Keywords: negative emissions, artificial carbon dioxide removal, Earth System modeling, carbon cycle, cumulative emissions, climate change

Supplementary material for this article is available online

Abstract

Artificial removal of CO_2 from the atmosphere (also referred to as negative emissions) has been proposed as a means to restore the climate system to a desirable state, should the impacts of climate change become ‘dangerous’. Here we explore whether negative emissions are indeed effective in reversing climate change on human timescales, given the potentially counteracting effect of natural carbon sinks and the inertia of the climate system. We designed a range of CO_2 emission scenarios, which follow a gradual transition to a zero-carbon energy system and entail implementation of various amounts of net-negative emissions at technologically plausible rates. These scenarios are used to force an Earth System Model of intermediate complexity. Results suggest that while it is possible to revert to a desired level of warming (e.g. 2 °C above pre-industrial) after different levels of overshoot, thermosteric sea level rise is not reversible for at least several centuries, even under assumption of large amounts of negative CO_2 emissions. During the net-negative emission phase, artificial CO_2 removal is opposed by CO_2 outgassing from natural carbon sinks, with the efficiency of CO_2 removal—here defined as the drop in atmospheric CO_2 per unit negative emission—decreasing with the total amount of negative emissions.

1. Introduction

Anthropogenic climate change has been shown to be irreversible on centennial to millennial timescales even after a complete cessation of CO_2 emissions [1–7]. While global mean temperature remains constant for many centuries after cessation of CO_2 emissions [2–4], the ongoing regional changes in temperature and precipitation are potentially substantial [2–5] and the thermosteric sea level continues to rise [2–6]. These findings imply that a net removal of anthropogenic CO_2 from the atmosphere (also referred to as ‘negative emissions’) may be necessary to reverse undesirable climate changes on timescales relevant to human civilization.

Recent studies [8–14] have explored the response of the climate system to negative emissions under idealized scenarios. Studies [10] and [11] assume an instantaneous removal of all anthropogenic CO_2, study [12] prescribes a 1% per year decrease in atmospheric CO_2 concentrations from quadrupled pre-industrial CO_2 levels, while study [13] prescribes a decline in CO_2 concentrations that mirrors atmospheric CO_2 in the Representative Concentration Pathways (RCPs) [15]. Generally, these studies show that while the mean land surface temperature responds promptly to the decrease in CO_2 concentrations, temperature over the ocean and thermosteric sea level (driven by thermal expansion of the ocean) exhibit a time lag in their response [12]. Globally, the decline in atmospheric CO_2 does not result in a simultaneous decrease in temperature to pre-industrial levels, as the heat stored in the oceans continues to be released for centuries onward [9–11]. Other climate system components, such as global sea ice area, also exhibit a lag in their responses, as they follow the temperature trajectory [12, 13]. The idealized scenarios considered in these studies require implementation of large amounts of negative CO_2 emissions [9–13], which likely exceed constraints on the scale and rate of implementation of these technologies [16, 17].

Several artificial CO_2 removal technologies have been proposed [18–22]. A first group includes land-based methods such as reforestation, afforestation and bio-energy production with carbon capture and storage (BECCS) [20]. Other options include technologies that capture CO_2 directly from ambient air [19], methods to enhance carbon uptake by natural sinks (e.g. ocean fertilization) and biochar [18]. None of the technologies have yet been applied at a large scale. Land-based methods are constrained by the availability of land for afforestation and biomass production. In particular, large-scale biomass production for BECCS raises food security concerns, as it may compete with biomass needed for food production and feedstock supply chains [18]. For CO_2 removal technologies involving carbon capture and storage (e.g. BECCS, direct air capture), concerns related to safe storage of captured CO_2 (usually in geological structures) also need to be considered.

The purpose of this study is to explore the reversibility of anthropogenic climate change and the carbon cycle response using a set of emission scenarios, which follow a gradual transition from a fossil-fuel driven economy to a zero-emission energy system with implementation of net negative CO_2 emissions. We expand on previous work by using plausible emission scenarios, which meet constraints related to the rate and scale of implementation of negative emissions derived from the integrated assessment literature. In contrast to previous studies, the focus of our study is not on the restoration of a pre-industrial climate, but rather on the return to a target level after overshoot, placing the analysis in the context of the discussion about the attainability of the 2 °C target. Also, this study is the first to present a detailed analysis of the global and regional carbon cycle response to various amounts of net negative emissions.

2. Methods

2.1. CO_2 emissions scenarios

In the scenario literature, few scenarios exist which entail *net* negative CO_2 emissions [22]. Most of these scenarios extend only to the year 2100, making it difficult to explore the long-term climate and carbon cycle response to a range of net negative emissions. To overcome these limitations, we designed a set of emission scenarios that follow a gradual transition to a zero-carbon energy system by 2100 and entail implementation of various amounts of net negative emissions between years 2100 and 2200.

To ensure the plausibility of CO_2 emission pathways used in this study, we designed them to meet several constraints derived from the integrated assessment literature. Firstly, to allow for a smooth transition from a current fossil-fuel based economy to a zero-emission energy system, while meeting the 2 °C temperature stabilization target, fossil fuel CO_2 emissions are required to peak between 2010 and 2030 and reach zero-emission level by 2100 [17, 23]. If the peak occurs at a later time, the rate of emission reductions required to reach zero emissions by 2100 would need to be steeper. Secondly, the maximum rate of CO_2 emission reductions is limited to 4% (with respect to year 2000 emissions, considering fossil fuel emissions only), as higher reduction rates are considered extreme based on the scenario literature [17, 23]. To allow for the possibility of higher emission reduction rates we performed a sensitivity analysis with reduction rates up to 6%. The maximum rate of CO_2 emission reductions is constrained by technological progress in developing clean energy and, potentially, negative emission technologies and the rate of introduction of these technologies to the current energy system. Thirdly, the total amount of negative emissions implemented is limited to a maximum of 550 GtC [20]. This limit is based on the capacity for geologic storage of CO_2. Estimates of the total global geologic CO_2 storage capacity range from 550 GtC to 1900 GtC [16]. We have chosen a value at the lower end of this range as these estimates do not account for technological feasibility, economic costs and social acceptability of CO_2 storage. Recognizing that our limit for the storage of CO_2 may be too restrictive, we designed an additional set of emission scenarios with negative cumulative emissions of up to 680 GtC (corresponding to removal of all anthropogenic CO_2). If negative emissions will be achieved with BECCS, which is considered the most cost-effective way of artificially removing CO_2 from the atmosphere [16, 18], another constraint arises due to the limited availability of land for biomass production. This constraint imposes a limit on the rate of CO_2 capture, with peak rates of CO_2 removal in integrated assessment studies ranging from 2.7 GtC yr^{-1} to 5.4 GtC yr^{-1} [16]. For direct air capture, the maximum rate of CO_2 removal is estimated to be somewhat higher—up to 9.5 GtC yr^{-1} [16]. In our study, the maximum rate of negative emissions is 6 GtC yr^{-1} in our standard scenarios, and 13.8 GtC yr^{-1} in the additional scenarios with extreme negative cumulative emissions.

Based on these constraints we designed two sets of emissions scenarios: Constant Cumulative Emissions (CCE) and Variable Cumulative Emissions (VCE) scenarios (figures 1(a) and 2(a); supplementary table S1). The net cumulative CO_2 emission target for the CCE scenarios is 550 GtC (including fossil-fuel and land-use emissions) over the period 2001–3000, which is compatible with limiting global warming to 2 °C relative to pre-industrial in the UVic ESCM [24]. The scenarios differ in the peak fossil fuel emissions (between 10 and 14 GtC yr^{-1}), the year of peak emissions (between 2017 and 2029) and, accordingly, the amount of negative emissions implemented (0 to 305

GtC removed), to reach the same cumulative emission target (supplementary table S1). The VCE scenarios entail fossil fuel emissions that peak at 12 GtC yr^{-1} in 2025, followed by implementation of different amounts of negative emissions (0 to 460 GtC removed), reaching different amounts of cumulative emissions over the period 2001–3000, in the range of 200–700 GtC (supplementary table S1). For both scenario sets (CCE and VCE), we assume that net negative emissions are implemented in the period 2100–2200 (with slight variations depending on scenario), followed by zero CO_2 emissions during 2200–3000. Both scenario sets include a reference zero-emission pathway, where emissions peak and decline to zero without implementation of negative emissions. Note that we make assumptions only about the *net* CO_2 emissions. For instance, our scenarios include cases where negative CO_2 emissions are phased in before 2100, but are smaller than positive emissions. Similarly, zero emissions after 2200 could be achieved with a positive emission floor associated with irreducible emissions e.g. from food production, which is offset by negative emissions. The physical effects of land-use changes (LUC) potentially associated with negative emissions (if they were implemented as BECCS, for instance) are not considered.

2.2. Model description

This study uses the University of Victoria Earth System Climate Model (UVic ESCM, version 2.9), a model of intermediate complexity with a horizontal grid resolution of 1.8°(meridional) × 3.6°(zonal) [1]. The physical model consists of a simplified atmospheric model coupled to a general circulation ocean model and a dynamic-thermodynamic sea-ice model [25]. The atmosphere is represented by a single layer energy-moisture balance model, where advection and diffusion are responsible for horizontal transport of temperature and moisture, and includes parameterization of dynamical feedbacks [25]. The atmospheric model is coupled to a three-dimensional ocean general circulation model (the Geophysical Fluid Dynamics Laboratory Modular Ocean Model) with 19 vertical levels [25]. The ocean general circulation model is coupled to a sea-ice model, which includes thermodynamic components (open water sea ice) as well as elastic-viscous dynamics [25]. Ocean biogeochemistry is represented in terms of an inorganic ocean carbon model (following the Ocean Carbon-Cycle Model Intercomparison Project protocols [26]) and a NPZD (nutrient, phytoplankton, zooplankton, detritus) model of ocean biology [27]. The model also includes carbonate dissolution in ocean sediments [1]. Furthermore, the UVic model includes a land surface model based on the Hadley Centre Met Office Surface Exchange Scheme coupled to a dynamic terrestrial vegetation model, the Top-down Representation of Interactive Foliage and Flora including Dynamics model [1, 28].

2.3. Model experiments

We performed a common simulation for the historical period (1801–2000), followed by a range of future simulations forced with the CO_2 emission scenarios described above. In the historical simulation, atmospheric CO_2 was prescribed according to its observed evolution. The historical run also includes natural forcings (volcanic and solar), and forcing from non-CO_2 greenhouse gases (GHGs) and sulphate aerosols, following observations-based values for the period 1801–2000. The year-2000 model configuration from the historical run was used to initialize the CCE and VCE scenario-driven simulations. These simulations also include CO_2 emissions from LUC, which follow scenario RCP 2.6 [15] to the year 2100 and are then linearly extrapolated to reach zero in the year 2150. Total LUC emissions over the period 2001–2150 are 80 GtC. In addition to CO_2 emissions from fossil fuels and LUC, all CCE and VCE simulations include radiative forcing from sulphate aerosols and non-CO_2 GHGs. Both forcings follow observations-based values until the year 2010 (when the two forcings nearly cancel each other), and are held fixed at the year-2010 value thereafter. To explore the sensitivity of the climate and carbon cycle response to this assumption, we conducted additional simulations with sulphate and non-CO_2 greenhouse gas radiative forcing from RCP 2.6 [15].

3. Results and discussion

3.1. Physical climate system response

In the CCE simulations, the atmospheric CO_2 concentration peaks between years 2070 and 2080 at 470–555 ppm (figure 1(b)). After the peak, CO_2 concentration decreases, with larger rates of decline for pathways with greater amounts of negative CO_2 emissions during the period 2100–2200. After CO_2 emissions reach zero, the decrease in atmospheric CO_2 slows, being entirely driven by ocean CO_2 uptake (figure 3(d)).

Global mean temperature peaks between years 2100 and 2170 at values ranging from about 2.0 °C to 2.5 °C (relative to 1800) for the different scenarios (figure 1(c)). During the negative emissions phase, temperature decreases rapidly, particularly for scenarios with large negative CO_2 emissions, attaining a warming of 2.0 °C at year 2200. After emissions reach zero (in year 2200), temperature continues to decline slightly, consistent with results from earlier studies [2–4]. Pathways with higher peak emission rates and larger amounts of CO_2 removal attain the same warming after year 2200 as the reference pathway with a lower peak emission rate and no negative emissions. This is consistent with the finding that the warming after

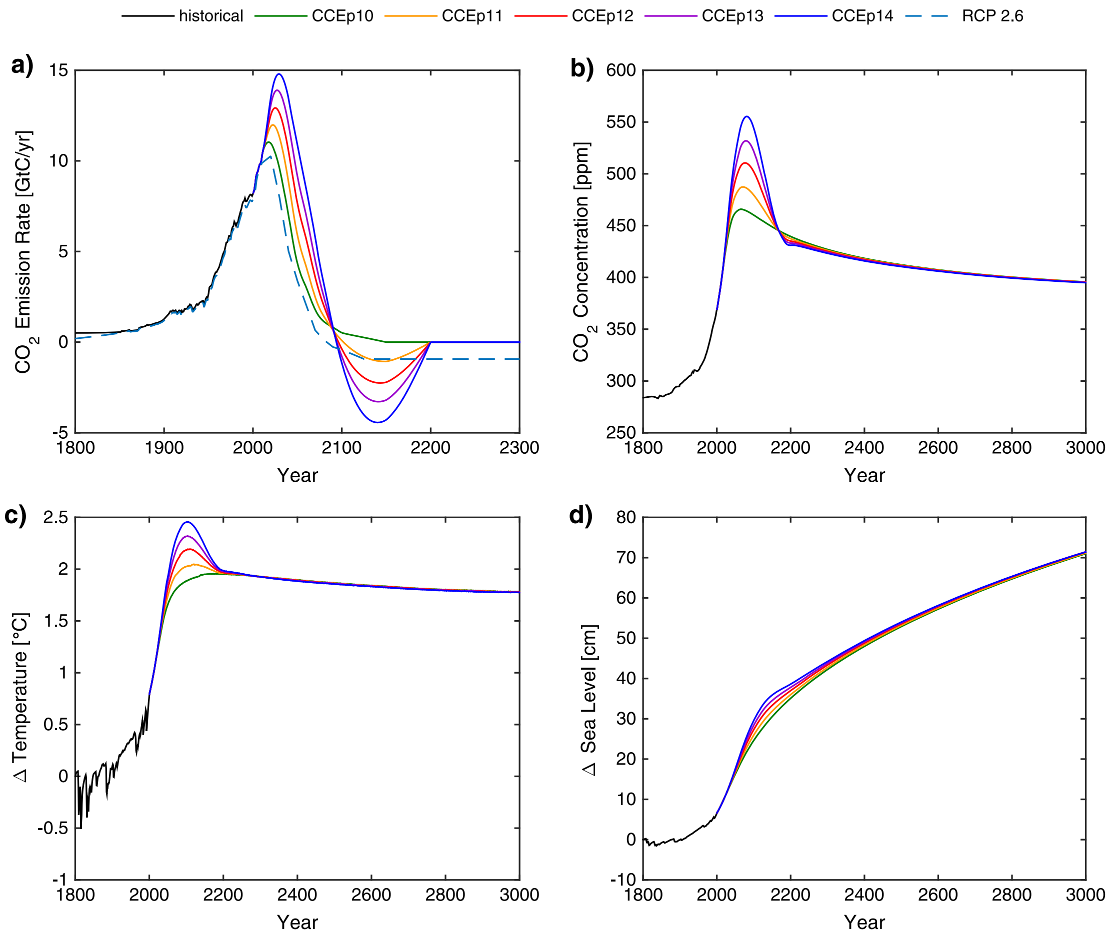

Figure 1. Time series of global variables for constant cumulative emissions (CCE) simulations. (a) CO_2 emission rate (fossil fuel and land use change) (b) atmospheric CO_2 concentration; (c) global mean temperature change relative to 1801; (d) thermosteric sea level rise relative to 1801. Scenario names in the legend indicate peak fossil fuel emission rate (in GtC yr^{-1}). RCP 2.6 in panel (a) is shown for reference.

cessation of CO_2 emissions is independent of emission pathway and determined solely by the amount of cumulative emissions (550 GtC between years 2001 and 2200) [29–31].

Our results indicate that compared to a scenario with zero emissions, implementation of net negative emissions allows for a faster reversal of global mean temperature from peak levels. Specifically, our results suggest that it is possible to revert to a warming of 2 °C on centennial timescales after different levels of overshoot, given the assumptions about the rate and scale of deployment of negative emission technologies used in this study.

Sea level rise due to ocean thermal expansion (thermosteric sea level rise) continues in all scenarios despite the implementation of net negative emissions (figure 1(d)). The rate of sea level rise slows between 2100 and 2200 for scenarios with large negative emissions, but rebounds after emissions return to zero in year 2200 (supplementary figure S1(a)). When emission pathways converge at year 2200, thermosteric sea level rise is about 4 cm higher in the scenario with the highest peak emission rate relative to the reference scenario without negative emissions, indicating slight path dependence associated with ocean thermal inertia [8, 32]. By 2500, the rate of sea level rise is similar in all scenarios (supplementary figure S1(a)).

A second set of simulations (VCE simulation) was performed to explore whether scenarios with larger removal of CO_2 from the atmosphere (up to 460 GtC) could lead to stabilization and potentially even reversal of sea level rise. In these simulations, atmospheric CO_2 decreases from a peak value of 510 ppm to 360–440 ppm during the negative emissions phase (2100–2200), and global mean temperature stabilizes at 1.2 °C to 1.8 °C above pre-industrial levels (figures 2(b) and (c)). We find that despite implementation of large amounts of negative emissions, sea level continues to rise, albeit at a slower rate compared to the reference case without negative emissions (figure 2(d); supplementary figure S1(b)). The rate of sea level rise declines rapidly between 2100 and 2200 for scenarios with large negative emissions, but slightly increases and stabilizes as soon as artificial CO_2 removal ceases (supplementary figure S1(b)). To stabilize sea level at a desired (low) level, a continued removal of CO_2 from the atmosphere would be required to lower the atmospheric CO_2 concentration

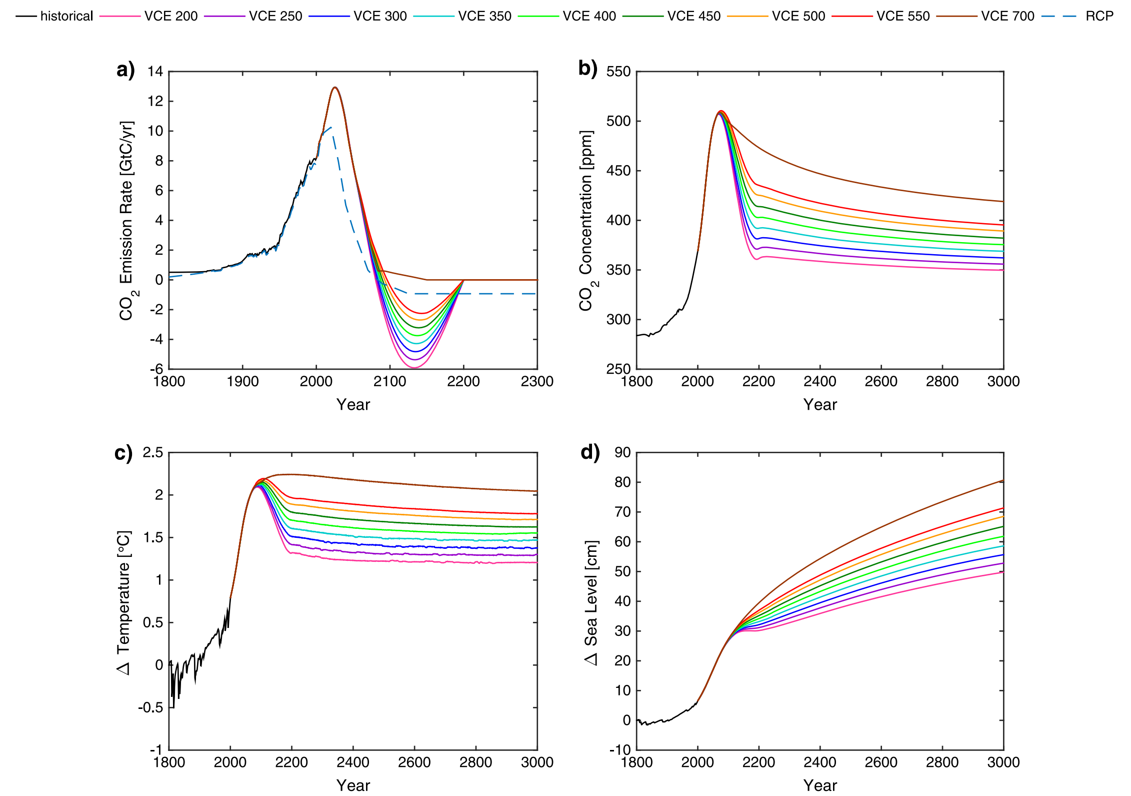

Figure 2. Time series of global variables for variable cumulative emissions (VCE) simulations. (a) CO_2 emission rate (fossil fuel and land use change) (b) atmospheric CO_2 concentration; (c) global mean temperature change relative to 1801; (d) thermosteric sea level rise relative to 1801. Scenario names in the legend indicate net cumulative total (fossil fuel and land use change) CO_2 emissions since 2001 (in GtC). The fossil fuel CO_2 emission rate for VCE Simulations peaks at 12 GtC yr^{-1} in all simulations. Note: scenario VCE550 is the same as CCEp12. RCP 2.6 in panel (a) is shown for reference.

and associated radiative forcing sufficiently to offset the warming effect from ocean thermal inertia. As opposed to the CCE pathways, the VCE pathways entail different amounts of cumulative emissions, and results in different magnitudes of thermosteric sea level rise by the year 3000.

Additional model simulations with larger total net negative emissions indicate that atmospheric CO_2 and associated radiative forcing would need to return to pre-industrial levels for sea level to fall and stabilize in the long term (supplementary figure S2). Analysis of the energy balance terms indicates that thermosteric sea level rise is closely linked to the time-integrated top-of-atmosphere (TOA) radiative flux (supplementary figure S3). Thus, a decline and stabilization of sea level is only possible if the TOA radiative flux is zero or negative (i.e. to outer space), implying zero or negative ocean heat uptake. In our simulations this is the case if the atmospheric CO_2 concentration is returned to pre-industrial levels; for a lower drop in atmospheric CO_2 ocean heat uptake becomes positive again after emissions are set to zero resulting in continued thermosteric sea level rise. Our finding that atmospheric CO_2 needs to be returned to pre-industrial concentrations for sea level to be reversed and stabilized permanently indicates that when emissions return to zero in 2200 the deep ocean is still in thermal equilibrium with pre-industrial atmospheric CO_2 (if it was in equilibrium with a higher atmospheric CO_2 level, it would release heat and sea level would drop if CO_2 was reduced beyond that level).

Thus, our findings suggest that reversal and stabilization of sea level on centennial timescales requires amounts of negative emissions beyond what is currently deemed to be technologically feasible. The version of the UVic ESCM used in this study does not include a dynamic ice sheet component and therefore does not account for sea level rise due to melting of ice (eustatic sea level rise). Due to the millennial response timescale of ice sheets, we expect that it would be even more challenging to reverse sea level rise if the eustatic component was considered.

In both the CCE and VCE simulations, we assumed that the future radiative forcing from non-CO_2 GHGs and sulphate aerosols nearly cancel each other. To test the effects of this assumption, we performed three VCE simulations (VCE 550, 350 and 200) with non-CO_2 GHG and sulphate aerosol forcing following the extended RCP 2.6 scenario until 2300, and held constant thereafter. Since the sulphate forcing decreases more rapidly than the non-CO_2 GHG forcing in RCP 2.6, and the total radiative forcing is larger, the global climate is warmer (by about 0.35 °C) for RCP 2.6 non-CO_2 GHG forcing. Key results such as the reversibility of global mean surface air temperature and the irreversibility of sea-level rise on

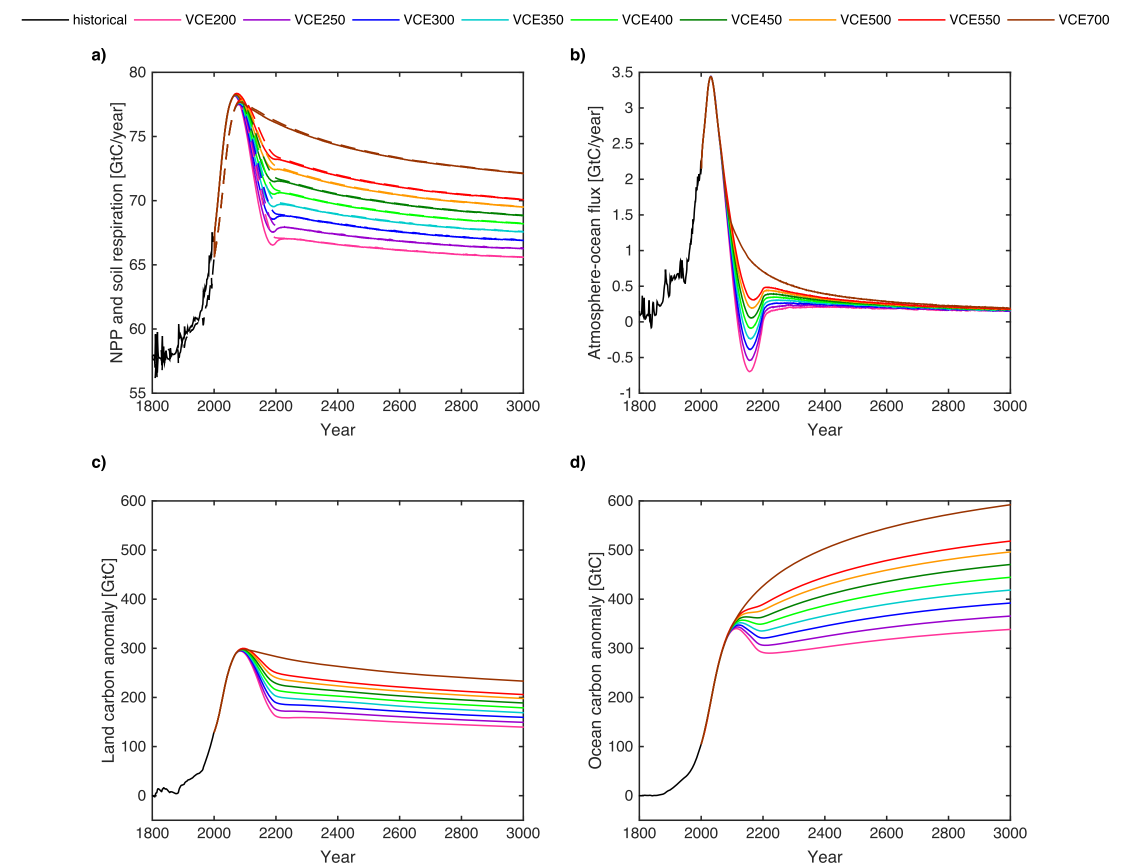

Figure 3. Time series of carbon fluxes and changes in carbon pools for the VCE simulations. Net primary productivity (NPP; solid lines) and soil respiration rate (dashed lines) (panel (a)); atmosphere-ocean flux (positive into the ocean; panel (b)); land carbon pool anomaly (panel (c)); ocean carbon pool anomaly (panel (d)). The difference between NPP and soil respiration is the atmosphere-land flux (positive into the land). Anomalies are relative to 1801. Note: panels (a) and (b) have different vertical scales.

centennial timescales, however, are unaffected by the different choice of non-CO_2 radiative forcing (supplementary figure S4).

Another uncertainty regards the equilibrium climate sensitivity. The standard equilibrium climate sensitivity of the UVic model is 3.6 °C. Sensitivity experiments with climate sensitivity values ranging from 1.5 °C to 4.5 °C again indicate that the degree of reversibility of global mean temperature and the irreversibility of sea level rise on centennial timescales are robust against the choice of equilibrium climate sensitivity (supplementary figure S5).

3.2. Carbon cycle response

Figure 3 shows the land and ocean carbon fluxes and pool anomalies for the VCE simulations. The change in the land carbon pool is driven by changes in the balance between net primary productivity (NPP) and soil respiration. During the positive emissions phase (until year 2100), both the ocean and the terrestrial biosphere take up CO_2. On land, the uptake is largely caused by the CO_2 fertilization effect, as elevated atmospheric CO_2 concentration levels enhance photosynthesis, leading to an increase in NPP (figure 3(a)). On the other hand, warmer temperatures lead to an increase in soil respiration rate; however, this effect is smaller than the increase in NPP, thereby leading to a net increase in carbon storage on land (figures 3(a) and (c)). Spatially, the Tropics and northern mid and high latitudes experience the largest increase in land carbon pool (figures 4(a) and (b)). At northern high latitudes, both elevated atmospheric CO_2 concentrations and higher temperature promote vegetation productivity, as the temperature gets closer to the optimal growth temperature in that region. In the Tropics, the temperature increase has a negative effect on vegetation productivity. Initially, this effect is overcompensated by a stronger CO_2 fertilization effect, but towards the end of the 21st century the negative effect of warming on vegetation productivity becomes large enough to tip the balance between NPP and soil respiration, resulting in CO_2 outgassing in the Tropics (figures 5(a) and (b)).

In the ocean, the uptake during the positive emission phase is associated with the increase in CO_2 partial pressure at the ocean-atmosphere interface, which drives a CO_2 flux into the ocean (figure 3(b)). Spatially, the atmosphere-ocean flux is positive in most regions, except for strong outgassing in the equatorial Pacific (figures 5(a) and (b)). The uptake is strongest in the tropical oceans (particularly the Eastern Tropical

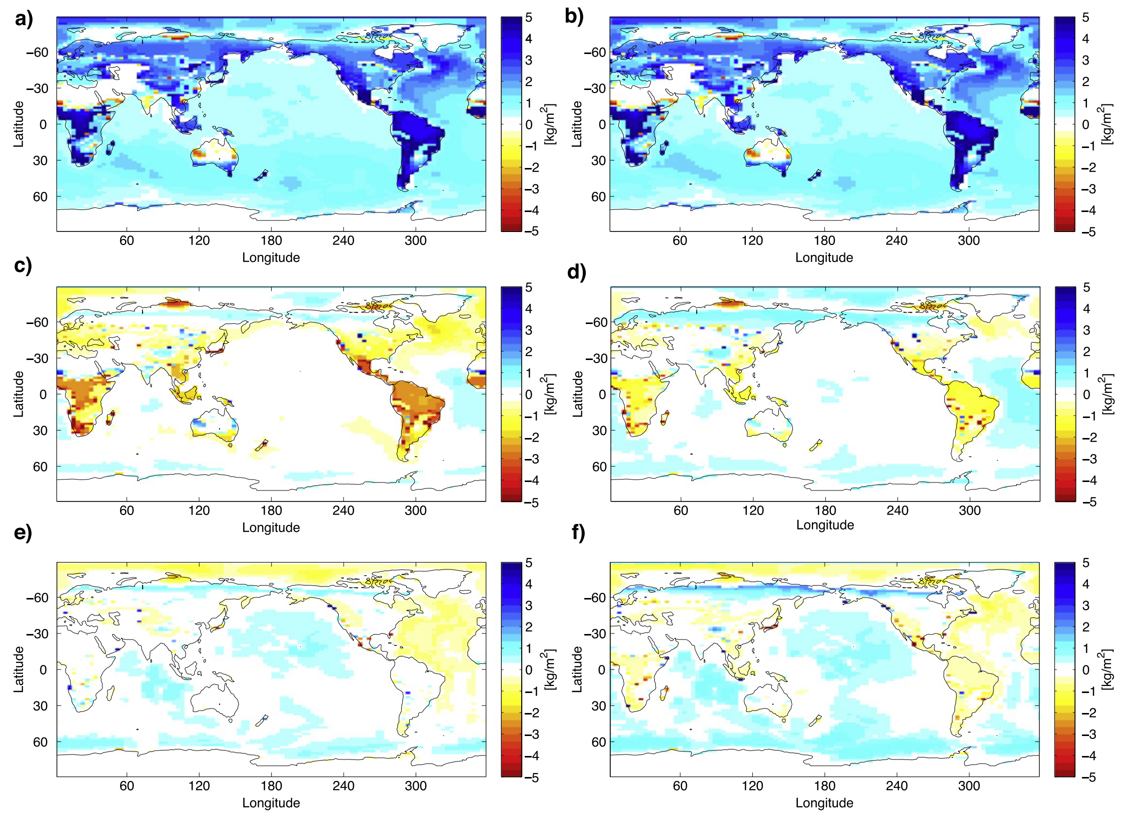

Figure 4. Spatial distribution of land and ocean carbon pool changes for VCE 200 (left) and VCE 550 (right) simulations. Top panels show changes over the positive emissions phase, middle panels show changes over the negative emissions phase and bottom panels show changes over the zero emissions phase. Differences are taken between decadal averages. (a) 2090–2100 minus 1800–1810 for VCE 200; (b) 2090–2100 minus 1800–1810 for VCE 550; (c) 2190–2200 minus 2090–2100 for VCE 200; (d) 2190–2200 minus 2090–2100 for VCE 550; (e) 2490–2500 minus 2190–2200 for VCE 200; (f) 2490–2500 minus 2190–2200 for VCE 550. Blue colors indicate an increase in carbon storage, whereas red colors indicate a decrease in carbon storage.

Pacific), the North Atlantic and the Southern Ocean. In the Eastern Tropical Pacific (both north and south of the Equator), warmer surface waters, aided by advection of nutrients from the equatorial upwelling system, enhance biological productivity, resulting in greater transport of carbon to deeper ocean layers, thereby increasing carbon uptake [33].

During the negative emission period (2100–2200), when atmospheric CO_2 starts to decline, both land and ocean outgas CO_2 into the atmosphere (figure 3). On land, declining atmospheric CO_2 levels lead to a decrease in NPP due to weaker CO_2 fertilization effect (figure 3(a)). Falling temperatures associated with the CO_2 decrease lead to a decline in soil respiration rates; however, this decline is slower than the decline in NPP (figure 3(a)). The reason is that NPP is largely controlled by atmospheric CO_2 whereas soil respiration is largely controlled by temperature, which lags the CO_2 decrease. As a result, there is a net release of CO_2 into the atmosphere and a decline in the land carbon pool (figure 3(c)). Regionally, the largest decline in terrestrial carbon occurs in the Tropics (figures 4(c) and (d)), primarily due to decline in atmospheric CO_2 levels and a weakening of the CO_2 fertilization effect. Although lower temperatures are beneficial for vegetation growth in the Tropics, the weakening of the CO_2 fertilization effect dominates and leads to outgassing of CO_2 (figures 5(c) and (d)). An opposite pattern prevails in the northern high latitudes, which see an increase in land carbon during the net-negative emission phase despite a decline in atmospheric CO_2 levels and decline in temperature in these regions (figures 4(c) and (d)). The carbon uptake in these regions occurs due to vegetation shifts, which lag the atmospheric CO_2 and temperature change due to the long (decadal to centennial) timescales involved. Boreal forest continues to expand in the northern high latitudes at the expense of shrubs, thereby increasing the carbon uptake in that region (supplementary figure S6). Globally, however, the carbon uptake in northern high latitudes during the negative emission phase is overcompensated by the total decline in land carbon in the Tropics.

In the ocean, the decrease in atmospheric CO_2 concentration levels caused by the net-negative emissions leads to outgassing of CO_2 for emissions pathways that entail large amounts of negative emissions (figure 3(b)). For example, the decrease in partial pressure for pathway VCE 200 is large enough to change the direction of the CO_2 flux and drive it away from the ocean. For pathways with a small amount of negative emissions (e.g. VCE 550), the flux remains positive

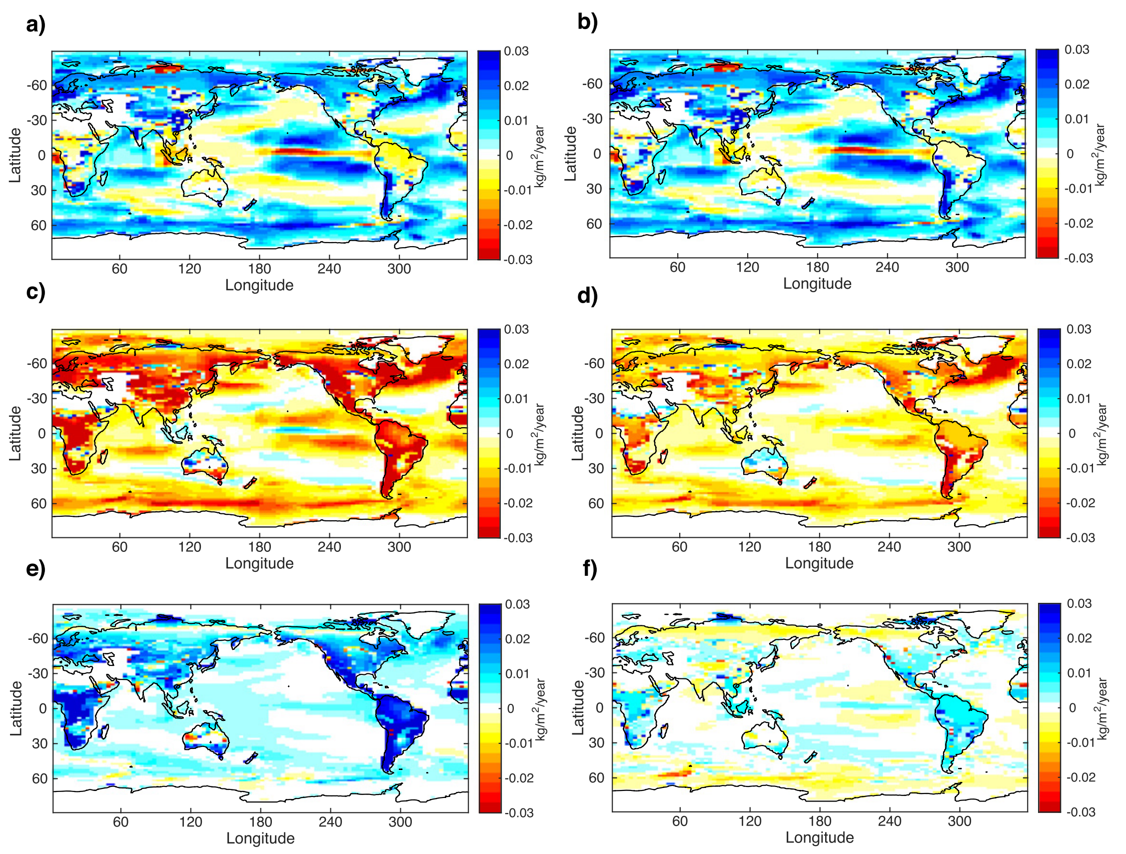

Figure 5. Changes in atmosphere-land and atmosphere-ocean carbon fluxes distribution for VCE 200 (left) and VCE 550 (right) simulations. Top panels show changes over the positive emissions phase, middle panels show changes over the negative emissions phase and bottom panels show changes over the zero emissions phase. Differences are taken between fifty-year averages. (a) 2050–2100 minus 1800–1850 for VCE 200; (b) 2050–2100 minus 1800–1850 for VCE 550; (c) 2150–2200 minus 2050–2100 for VCE 200 (d) 2150–2200 minus 2050–2100 for VCE 550; (e) 2450–2500 minus 2150–2200 for VCE 200; (f) 2450–2500 minus 2150–2200 for VCE 550. Flux changes are positive downward, i.e. into the land and the ocean. Blue colors indicate land and ocean carbon uptake, red colors indicate outgassing.

(into the ocean) but is much weaker than during the positive emissions phase. For pathways with large amounts of negative emissions, ocean carbon storage declines during the net-negative-emissions period (figures 3(b) and (d)). Spatially, during this period, the outgassing occurs mostly in the Southern Ocean, North Atlantic and tropical Pacific (figures 5(c) and (d)), i.e. the regions with the strongest CO_2 uptake during the positive emission phase. The pattern of outgassing is consistent with results from a previous study that used a more complex ocean model [32].

Once emissions return to zero (at year 2200), the decline in terrestrial carbon uptake slows or comes to a halt for emission pathways with lower total negative emissions (e.g. VCE 550, compared to VCE 200; figure 3(c)). At year 2500, land uptake ranges from 150 to 230 GtC, which corresponds to 23% to 25% of cumulative CO_2 emissions. Spatially, boreal forest coverage continues to expand in the northern high latitudes (supplementary figure S6), thereby leading to an increase in land carbon storage (figures 4(e) and (f)). After emissions return to zero at year 2200, the ocean turns again into a sink of atmospheric CO_2 (figures 3(b) and (d)). At year 2500, ocean uptake ranges from 310 to 460 GtC, which corresponds to 50% to 48% of cumulative emissions.

The carbon cycle response during the positive and negative emission phases is similar for the CCE simulations. The additional insight offered by those simulations is that the terrestrial and marine carbon cycle response after emissions reach zero in year 2300 is independent of emission scenario (supplementary figure S7), and determined only by the total cumulative emissions (550 GtC for all CCE scenarios). This suggests that the finding of previous studies that the carbon cycle response is pathway independent [9, 34], can be generalized to emission pathways entailing net negative emissions.

3.3. Efficiency of artificial CO_2 removal

Our analysis of the carbon cycle shows that efforts to artificially remove CO_2 from the atmosphere during the net-negative emissions period (years 2100–2200) are offset by outgassing of CO_2 from the natural carbon sinks. The larger the amount of net-negative emissions implemented, the stronger the outgassing from both the ocean and terrestrial biosphere. To quantify the effectiveness of the artificial CO_2 removal,

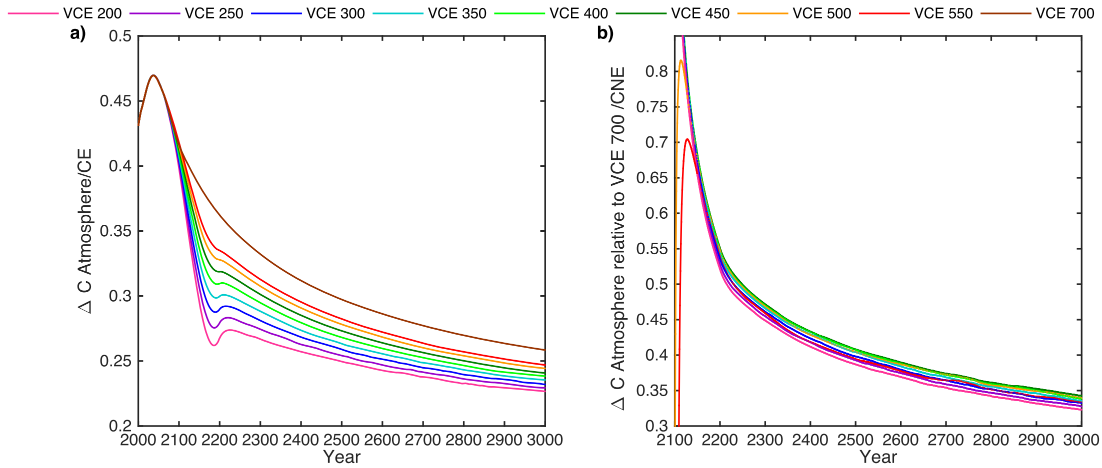

Figure 6. Efficiency of atmospheric CO_2 removal for VCE simulations. Ratio of atmospheric carbon burden change relative to year 1800 (ΔC Atmosphere) to cumulative CO_2 emissions (CE) (panel (a)); ratio of atmospheric carbon burden change relative to the VCE 700 simulation, to cumulative negative emissions (CNE) (panel (b)).

we define an efficiency measure as the ratio of the change in atmospheric CO_2 burden to cumulative CO_2 emissions (figure 6(a)). For positive CO_2 emissions, this measure is commonly referred to as the airborne fraction of cumulative emissions. We extend the usage of this term to negative emissions, noting that it has a different meaning: it indicates the drop in atmospheric CO_2 for a given amount of CO_2 removed, implying that the larger the airborne fraction, the larger the efficiency of negative emissions.

During the positive emissions phase (until year 2100), the airborne fraction (figure 6(a)) increases, peaks around year 2050 (the year of peak CO_2 emissions), followed by a decrease. During the net-negative emissions period in years 2100–2200, the airborne fraction continues to decrease, with a steeper decline for pathways with larger net-negative emissions (e.g. VCE 200). This indicates that the change in atmospheric CO_2 burden per unit CO_2 removed is smaller for pathway with larger net-negative emissions, implying a lower efficiency of CO_2 removal.

As indicated by the carbon cycle response to the reference zero negative emissions pathway VCE 700 (figures 2 and 3) part of the decline in atmospheric CO_2 during the negative emission phase is due to continued uptake of CO_2, as the carbon sinks equilibrate with past (positive) CO_2 emissions. To correct for this effect, we compute a modified efficiency measure as the ratio of the change in atmospheric CO_2 burden relative to the VCE 700 scenario to cumulative negative CO_2 emissions (figure 6(b), supplementary table S2). This measure indicates that in year 2200 about half of the negative emissions effectively result in a drop in atmospheric CO_2, with this fraction declining over time. Compared to the airborne fraction, the difference between scenarios is reduced (year-2200 range: 0.52–0.55). Interestingly, efficiency is highest for pathway VCE 450, with an intermediate amount of negative emissions, while efficiency is still lowest for the pathway with the largest amount of negative emissions (VCE 200).

4. Summary and conclusions

In summary, our study suggests that it is possible, in principle, to revert global mean temperature to 2 °C on centennial timescales after different levels of overshoot with the implementation of net negative emissions. However, sea level continues to rise for at least several centuries despite large amounts of CO_2 removed from the atmosphere. Only if atmospheric CO_2 is returned to pre-industrial levels, and the net radiative flux at the top to the atmosphere is zero or negative, will sea level start to fall and stabilize in the long term. During periods of net negative emissions, artificial CO_2 removal is opposed by CO_2 outgassing from marine and terrestrial carbon sinks, with the amount of outgassing increasing with the total amount of negative emissions. The efficiency of CO_2 removal —here defined as the change in atmospheric CO_2 per unit negative emission—decreases with increasing total amount of negative emissions.

Results of this study indicate that the long-term climate and carbon cycle response is the same for emissions pathways with an early and low CO_2 emission peak, followed by implementation of small amounts of negative emissions and pathways with a later and higher peak and large amounts of negative emissions. This implies that in view of stabilizing global mean temperature below 2 °C in the long-term, delays in reducing CO_2 emissions today could, in principle, be offset by negative emissions in the future. It needs to be considered, however, that pathways with higher peak emission rates entail larger peak warming, which increases the likelihood of crossing thresholds for 'dangerous' climate change.

The key results of our study are robust against the details of the CO_2 emission scenarios. Because of the path independence of the climate and carbon cycle response, variations in the timing and amount of peak CO_2 emissions, maximum emission reduction rate and total amount of negative emissions would not affect the long-term Earth System response as long as the net cumulative CO_2 emissions are the same.

Earth system responses not included in our analysis, such as sea level rise from melting ice sheets and permafrost-carbon cycle feedbacks, are expected to reduce the reversibility of anthropogenic climate change even further due to their long timescales. Restoration of the permafrost carbon pool in response to cooling has been estimated to take several centuries to millennia [13]. Therefore, consideration of permafrost feedbacks would likely slow the decline in atmospheric CO_2 (and thus, temperature), thereby reducing the efficiency of artificial CO_2 removal.

Our results suggest that while negative emissions, at the scale of deployment considered here, allow to restore global mean surface air temperature to a lower level, they are ineffective at reversing responses in climate system components with long response timescales such as thermosteric sea level rise. We conclude that while carbon dioxide removal may be a helpful tool in conjunction with other efforts aimed at reducing the rise in atmospheric CO_2, it is not a silver bullet to restore the climate system to a desirable state on timescales relevant to human civilization once the impacts of climate change turn out to be 'dangerous'.

Acknowledgments

We would like to thank Chris Jones and two anonymous reviewers for providing feedback on the manuscript. K Zickfeld acknowledges support from the Natural Sciences and Engineering Research Council Canada (NSERC) Discovery Grant Program.

References

[1] Eby M, Zickfeld K, Montenegro A, Archer D, Meissner K J and Weaver A J 2009 Lifetime of anthropogenic climate change: millennial time scales of potential CO_2 and surface temperature perturbations *J. Clim.* **22** 2501–11

[2] Gillett N P, Arora V K, Zickfeld K, Marshall S J and Merryfield W J 2011 Ongoing climate change following a complete cessation of carbon dioxide emissions *Nat. Geosci.* **4** 83–7

[3] Solomon S, Plattner G K, Knutti R and Friedlingstein P 2009 Irreversible climate change due to carbon dioxide emissions *Proc. Natl Acad. Sci. USA* **106** 1704–9

[4] Matthews H D and Caldeira K 2008 Stabilizing climate requires near-zero emissions *Geophys. Res. Lett.* **35** L04705

[5] Frölicher T and Joos F 2010 Reversible and irreversible impacts of greenhouse gas emissions in multi-century projections with the NCAR global coupled carbon cycle-climate model *Clim. Dyn.* **35** 1439–59

[6] Matthews H D and Zickfeld K 2012 Climate response to zeroed emissions of greenhouse gases and aerosols *Nat. Clim. Change* **2** 338–41

[7] Lowe J A, Huntingford C, Raper S C B, Jones C D, Liddicoat S K and Gohar K L 2009 How difficult is it to recover from dangerous levels of global warming? *Environ. Res. Lett.* **4** 014012

[8] Bouttes N, Gregory J M and Lowe J A 2013 The reversibility of sea level rise *J. Clim.* **26** 2502–13

[9] Zickfeld K *et al* 2013 Long term climate change commitment and reversibility: an EMIC intercomparison *J. Clim.* **26** 5782–809

[10] Cao L and Caldeira K 2010 Atmospheric carbon dioxide removal: long-term consequences and commitment *Environ. Res. Lett.* **5** 024011

[11] Held I M, Winton M, Takahashi K, Delworth T, Zeng F and Vallis G K 2010 Probing the fast and slow components of global warming by returning abruptly to preindustrial forcing *J. Clim.* **23** 2418–27

[12] Boucher O, Halloran P R, Burke E J, Doutriaux-Boucher M, Jones C D, Lowe J, Ringer M A, Robertson E and Wu P 2012 Reversibility in an Earth System model in response to CO_2 concentration changes *Environ. Res. Lett.* **7** 024013

[13] MacDougall A H 2013 Reversing climate warming by artificial atmospheric carbon-dioxide removal: can a holocene-like climate be restored? *Geophys. Res. Lett.* **40** 5480–5

[14] Cao L, Han Z, Meidi Z and Shuangjing W 2014 Response of ocean acidification to a gradual increase and decrease of atmospheric CO_2 *Environ. Res. Lett.* **9** 024012

[15] Vuuren D *et al* 2007 Stabilizing greenhouse gas concentrations at low levels: an assessment of reduction strategies and costs *Clim. Change* **81** 119–59

[16] Tavoni M and Socolow R 2013 Modeling meets science and technology: an introduction to a special issue on negative emissions *Clim. Change* **118** 1–14

[17] Elzen M J, Vuuren D and Vliet J 2010 Postponing emission reductions from 2020 to 2030 increases climate risks and long-term costs *Clim. Change* **99** 313–20

[18] McGlashan N, Shah N, Caldecott B and Workman M 2012 High-level techno-economic assessment of negative emissions technologies *Process Saf. Environ. Prot.* **90** 501

[19] Lackner K S, Brennan S, Matter J M, Park A-A, Wright A and van der Zwaan B 2012 The urgency of the development of CO_2 capture from ambient air *Proc. Natl Acad. Sci.* **109** 13156–62

[20] Azar C *et al* 2010 The feasibility of low CO_2 concentration targets and the role of bio-energy with carbon capture and storage (BECCS) *Clim. Change* **100** 195–202

[21] Shepherd J G 2012 Geoengineering the climate: an overview and update *Philos. Trans. A: Math. Phys. Eng. Sci.* **370** 4166–75

[22] Clarke L *et al* Assessing transformation pathways *Climate Change 2014: Mitigation of Climate Change Contribution of Working Group III to the Fifth Assessment Report of the Intergovernmental Panel on Climate Change* ch 6 in press

[23] Rogelj J *et al* 2011 Emission pathways consistent with a 2 °C global temperature limit *Nat. Clim. Change* **1** 413–8

[24] Zickfeld K, Eby M, Matthews H D and Weaver A J 2009 Setting cumulative emissions targets to reduce the risk of dangerous climate change *Proc. Natl Acad. Sci.* **106** 16129–34

[25] Weaver A J *et al* 2001 The UVic Earth System climate model: model description, climatology, and applications to past, present and future climates *Atmos.—Ocean* **39** 361–428

[26] Orr B J C 1999 On ocean carbon-cycle model comparison *Tellus* B **51** 509–30

[27] Schmittner A, Oschlies A, Matthews H D and Galbraith E D 2008 Future changes in climate, ocean circulation, ecosystems, and biogeochemical cycling simulated for a business-as-usual CO_2 emission scenario until year 4000 AD *Glob. Biogeochem. Cycles* **22** GB1013

[28] Meissner K J, Weaver A J, Matthews H D and Cox P M 2003 The role of land surface dynamics in glacial inception: a study with the UVic Earth System model *Clim. Dyn.* **21** 515–37

[29] Matthews H D, Gillett N P, Stott P A and Zickfeld K 2009 The proportionality of global warming to cumulative carbon emissions *Nature* **459** 829–32
[30] Allen M *et al* 2009 Warming caused by cumulative carbon emissions towards the trillionth tonne *Nature* **458** 1163–6
[31] Zickfeld K, Arora V K and Gillett N P 2012 Is the climate response to CO_2 emissions path dependent? *Geophys. Res. Lett.* **39** L05703
[32] Vichi M, Navarra A and Fogli P G 2013 Adjustment of the natural ocean carbon cycle to negative emission rates *Clim. Change* **118** 105–18
[33] Zickfeld K, Eby M, Matthews H D, Schmittner A and Weaver A J 2011 Nonlinearity of carbon cycle feedbacks *J. Clim.* **24** 4255–75
[34] Herrington T and Zickfeld K 2014 Path independence of climate and carbon cycle response over a broad range of cumulative carbon emissions *Earth Syst. Dynam.* **5** 409–22